Lasing Droplets: Highlighting the Liquid-Air Interface by Laser Emission

SHI-XIONG QIAN,* JUDITH B. SNOW,† HUEY-MING TZENG,‡ RICHARD K. CHANG

When dye-doped ethanol droplets are irradiated with an intense pulsed laser beam, the resulting laser emission from individual droplets highlights the liquid-air interface. Photographs of the lasing droplets in the micrometer size range taken in a single 10-nanosecond laser pulse clearly show the dynamic changes in droplet size, shape, and orientation.

THE PROPERTIES OF MICROMETER-sized droplets (microparticles) are important in the fields of atmospheric science, biology, combustion, and interfacial chemistry. Properties of interest include droplet size and shape, evaporation and condensation rates, details of the liquid-air interface, dynamic surface tension, viscosity, and chemical composition. Light scattering provides a nearly instantaneous, nonintrusive technique for investigating in situ both static and dynamic properties of an individual microparticle or an ensemble of microparticles. The scattered light may be at the same wavelength as the incident radiation (elastic scattering) or at a different wavelength (inelastic scattering). Traditionally, morphological properties of the microparticle are deduced from the angular dependence of the elastically scattered radiation at a given wavelength. Electronic and vibrational properties of the microparticle medium are obtained from the absorption spectrum or from the fluorescence or Raman spectrum of the inelastically emitted radiation.

Several investigators have reported the occurrence of spectrally narrow resonances in the light scattered from transparent or weakly absorbing microparticles (droplets and fibers) when the wavelength of the incident or wavelength-shifted radiation is such that the electromagnetic modes of the microparticle are excited (*1–4*). These resonances have been observed in elastic scattering (*1*), spontaneous Raman scattering (*2*), fluorescence (*3*), and optical levitation spectroscopy (*4*). Regardless of whether the scattering is elastic or inelastic, coherent or incoherent, these resonances have been referred to as surface waves, "whispering gallery" modes, or morphology-dependent resonances (MDR's). The wavelengths at which these resonances occur (regardless of the scattering process) can be predicted from the well-established theories for elastic scattering from dielectric cylinders and spheres (*5*). The position of these MDR's depends on the size parameter ($x = 2\pi a/\lambda$, where a is the radius and λ is the wavelength) and on the relative refractive index ($m = n/n_0$, where n and n_0 are the refractive indices of the microparticle and the surrounding medium, respectively.)

MDR's result whenever a light wave inside the microparticle, upon undergoing high internal reflection at the interface, has the same phase at the completion of one round trip as at the beginning. Upon irradiation by a monochromatic plane wave, the spherical or cylindrical interface can couple two counterpropagating waves within the circumference. For specific incident wavelengths commensurate with the natural resonant modes of the microparticle, these two counterpropagating waves can result in a standing wave of greatly enhanced internal field strength that is confined near the interface (*6, 7*). Such resonances are referred to as input resonances. Whenever the wavelength of the internally generated, inelastic radiation corresponds to a MDR, it is described as an output resonance. For the internally generated wavelength-shifted radiation, the interface acts as an optical cavity and provides optical feedback as that particular wave travels around the circumference. We have observed nonlinear optical phenomena in micrometer-sized droplets irradiated with a laser beam (*8, 9*). Both stimulated Raman scattering (SRS) spectra from water droplets and ethanol droplets (*8*) and laser emission spectra from dye-doped droplets (*9*) were observed with a pump laser of very low intensity. Here we present photographs of lasing droplets of different shapes and sizes.

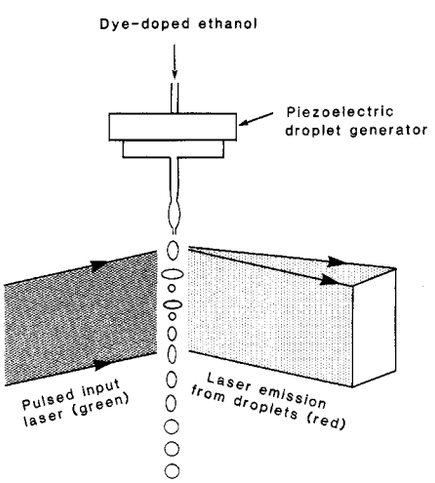

Fig. 1. Schematic diagram of experimental apparatus for detecting laser emission from the droplet stream. A cylindrically focused sheet of green laser light irradiates a portion of the droplet stream. The excited droplets isotropically emit partially polarized red laser and orange fluorescence radiation, a portion of which is imaged onto either a camera or a spectrograph.

The red dye–doped (rhodamine 590 or rhodamine 640) ethanol droplets were generated with a modified Berglund-Liu piezoelectric vibrating-orifice aerosol generator (*10*) with a 20- to 35-μm aperture that produced a linear stream of highly monodisperse, closely spaced droplets. The radii of the droplets could be varied from 20 to 40 μm by changing the frequency of the oscillator (30 to 70 kHz) driving the piezoelectric orifice. The green second-harmonic radiation (532 nm, 10-nsec pulse width) of a Nd:YAG (neodymium-doped yttrium iron garnet) laser was used to irradiate the droplet stream (Fig. 1).

The droplets were photographed with a microscope in conjunction with a standard 35-mm SLR camera on either ASA 400 or 1000 color film. A red optical filter placed between the camera and the droplets blocked the green incident radiation from the droplets, permitting only the red laser emission and orange fluorescence from the droplets to expose the film. Photographs (Figs. 2 and 3) that show the green radiation were taken without the red optical filter. The photographs containing both the green incident and red laser emission radiation were taken with a polarization analyzer. Since the green radiation from the droplet is predominately polarized, crossed polarizers greatly diminish this image. The red laser emission was not totally polarized. Most of the photographs were taken in a single 10-nsec pulse of the green incident beam. Consequently, the much weaker orange fluorescence is not observed.

Laser emission occurs when the gain around the circumference of the droplet exceeds the loss resulting from absorption and radiation leakage from the droplet. The laser emission spectrum of ethanol droplets containing rhodamine 590 is shown in Fig. 4. In spectral region A (580 to 590 nm),

Section of Applied Physics and Center for Laser Diagnostics, Yale University, New Haven, CT 06520.

*On leave from the Department of Physics, Fudan University, Shanghai, People's Republic of China.
†Present address: Naval Underwater Systems Center, New London Laboratory, New London, CT 06320.
‡Present address: IBM Research Laboratory, San Jose, CA 95123.

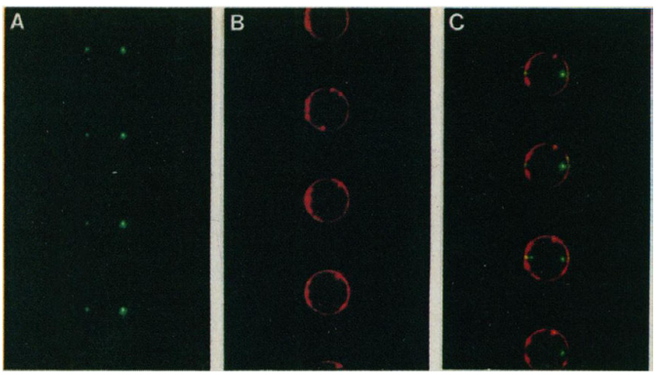

Fig. 2 (left). Photographs of a stream of droplets irradiated by a single 10-nsec laser pulse. (A) Two green spots resulting from the green incident radiation (elastic scattering) visible at only the front and back interfaces. (B) Red laser emission occurring throughout the liquid-air boundary (red filter used). (C) Simultaneously detected red laser emission and green radiation scattered by the droplet (crossed polarization analyzer used). The green incident pump radiation is propagating from left to right. Fig. 3 (right). A series of photographs of laser emission from the droplet stream within the first few millimeters of the vibrating orifice. (A) The upper portion of the stream showing the periodically perturbed, continuously connected liquid cylinder and the development of separate, highly distorted droplets. (B) The lower portion of the stream, showing the transition from oscillating prolate-to-oblate spheroids to a stream of monodisperse, equally spaced spherical droplets. (C) A photograph of combined laser emission (red) and elastic scattering (green) shown for comparison. The yellow color is an artifact of the film when exposed to both red and green radiation. The incident green pump radiation is propagating from left to right.

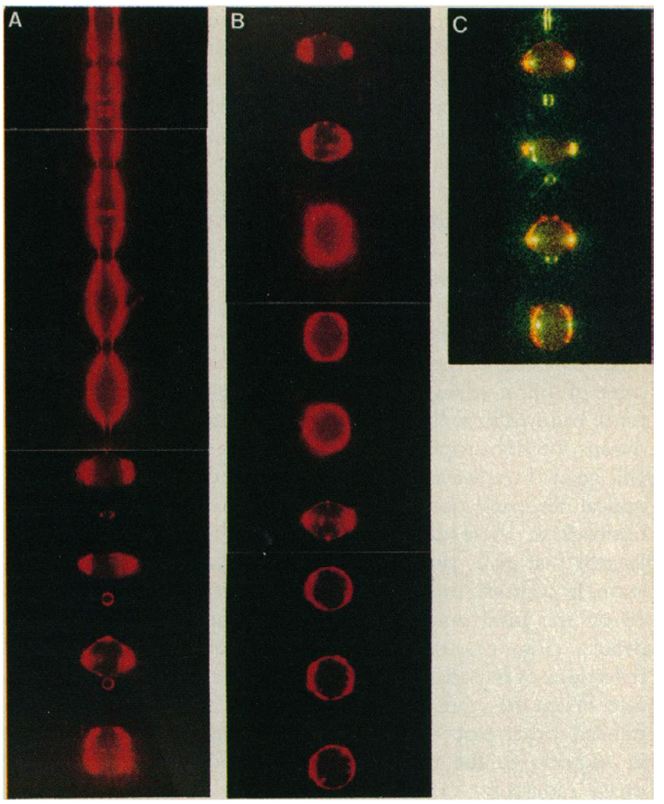

substantial absorption inhibits laser emission from the droplets. Region B (590 to 600 nm) is still somewhat absorbing since the absorption tail extends into the shorter wavelength portion of region B. However, in the longer wavelength portion of region B and in all of region C (600 to 610 nm), where absorption losses are progressively decreasing, the round-trip gain can exceed the loss. The pronounced onset of laser emission from the droplets occurs at approximately 595 nm (Fig. 4), demarcating the nonlasing and lasing regions. As in a typical dye laser, the lasing radiation from the droplet is red-shifted relative to the normal fluorescence spectrum.

The lasing droplets can be compared to a typical laser-pumped dye laser, for which the optical feedback is provided by external mirrors. For the lasing droplet, the optical feedback is provided by the high internal reflection at the spherical liquid-air boundary. The periodically spaced peaks in the emission from the droplet (arrows in Fig. 4) can be attributed to MDR's of different modes that are usually specified by their mode number and mode order. The occurrence of these peaks within the normally smooth bandwidth of the dye gain curve is a consequence of the droplet morphology only (the shape, size, and refractive index discontinuity at the interface) and does not correspond to any discrete vibrational transitions in the dye molecules themselves. For a conventional dye laser with external mirrors, the longitudinal cavity mode spacing is $\Delta\lambda = \lambda^2/2d$, where d is the distance between the front and rear reflectors. The mode spacing for the spherical droplet, in the asymptotic limit for large x, has values given by (*11*)

$$\Delta\lambda = (\lambda^2/2\pi a)\Delta x$$

where

$$\Delta x = \frac{\tan^{-1}(m^2 - 1)^{1/2}}{(m^2 - 1)^{1/2}}$$

Such a simple relation has enabled rapid and accurate determination of droplet size or size changes (or both) from the laser spectra of spherical droplets. Changes as small as 7×10^{-4} μm in radius have been measured (*10*) on the basis of the wavelength shifts of the MDR's in the laser emission from evaporating droplets ($a = 30$ μm). In principle, it is possible to determine radius changes as small as 1 part in 5×10^5 (*12*). Laser-induced shape distortions of individual droplets, resulting from nonuniform internal heating of the droplets, can be detected by monitoring the wavelength variation of the MDR's in the lasing spectrum (*13*). As the laser-perturbed droplets undergo small oscillations between prolate and oblate spheroids (axial ratio of 5 parts in

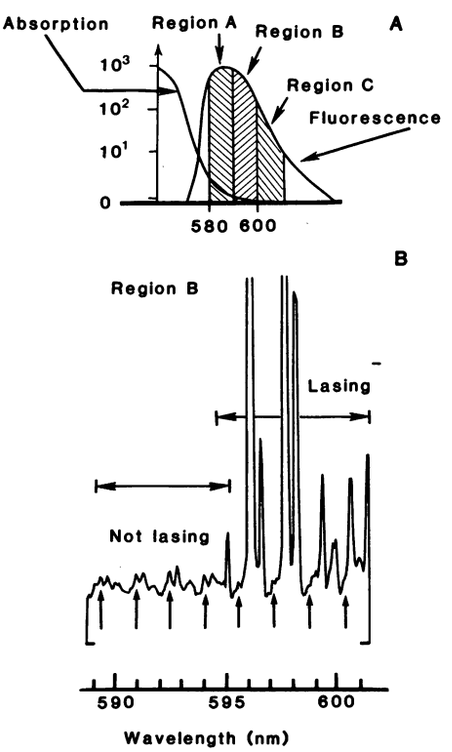

Fig. 4. (A) Schematic representation of the absorption and emission spectra of ethanol containing rhodamine 590. (B) The combined fluorescence and laser emission spectrum of the corresponding 30-μm-radius droplets for region B (590 to 600 nm). The MDR's, which have nearly equal wavelength spacing (arrows), are superimposed on the broad fluorescence background (*9*).

10^4) (*14*), the spectral positions of the MDR's oscillate as well. The observed oscillation frequency and damping constant for the resonance peak positions have been used to determine the dynamic surface tension and viscosity for flowing droplets (*13*).

The occurrence of the red laser emission at the spherical liquid-air boundary (Fig. 2) clearly demonstrates that optical feedback is confined near the surface, confirming the surface nature of the output resonance. As discussed earlier, the broadband fluorescence emission of the laser dye ensures that some of the wavelengths within the fluorescence bandwidth will satisfy resonance conditions for any droplet morphology, and it will be at those wavelengths that enhanced optical feedback occurs. It is the optical feedback at these different specific wavelengths that gives rise to the lasing surface wave. In contrast, the two green spots located on the front and back surfaces of the droplet (Fig. 2) result from the specular reflections of incident radiation at the interface. When the input resonance condition is fulfilled, other parts of the droplet interface in addition to the two spots will exhibit green radiation (*4*). However, since the incident laser radiation is monochromatic, the input resonance condition can be satisfied only for specific droplet sizes and shapes. In contrast, since the laser emission is broadband, the output resonance condition can always be satisfied for all sizes and shapes, as Figs. 2 and 3 indicate.

The surface-wave nature of the laser emission provides a novel means for observing droplets of different sizes and shapes and particularly for highlighting their liquid-air interface. Photographs of a droplet stream within the first few millimeters of the orifice exit are shown in Fig. 3. The droplets are generated from a cylindrical stream of liquid that is periodically pinched off by the vibrating orifice. The highly distorted droplets evolve into more regular and discrete spheroids that undergo a series of shape oscillations, becoming alternately prolate and oblate. Farther downstream from the orifice, surface tension forces the droplets to become essentially spherical (Fig. 2). The details of the evolution from a cylindrical stream to spherical droplets, particularly the interfacial regions, are highlighted by laser emission from all irradiated portions of the droplet stream. As seen in Fig. 3, it is clearly not necessary that the droplets be spherical or of a particular size for laser emission to be achieved. Laser emission is also present in the much smaller satellite droplets and in the cylindrical necking regions of the droplet stream (Fig. 3).

Regardless of the highly distorted droplet shape and size, near-field photographs demonstrate that laser emission highlights the liquid-air interface. Such laser emission photographs can provide a novel technique to study droplet dynamics.

REFERENCES AND NOTES

1. A. Ashkin and J. M. Dziedzic, *Appl. Opt.* **20**, 1803 (1981); J. F. Owen, P. W. Barber, B. J. Messinger, R. K. Chang, *Opt. Lett.* **6**, 272 (1981).
2. R. E. Benner, P. W. Barber, J. F. Owen, R. K. Chang, *Phys. Rev. Lett.* **44**, 475 (1980).
3. J. F. Owen, R. K. Chang, P. W. Barber, *Aerosol Sci. Technol.* **1**, 293 (1982); R. Thurn and W. Kiefer, *Appl. Spectrosc.* **38**, 78 (1984).
4. A. Ashkin, *Science* **210**, 1081 (1980).
5. M. Kerker, *The Scattering of Light and Other Electromagnetic Radiation* (Academic Press, New York, 1969); C. F. Bohren and D. R. Huffman, *Absorption and Scattering of Light by Small Particles* (Wiley, New York, 1983).
6. J. F. Owen, R. K. Chang, P. W. Barber, *Opt. Lett.* **6**, 540 (1981).
7. A. B. Pluchino, *Appl. Opt.* **20**, 2986 (1981).
8. J. B. Snow, S.-X. Qian, R. K. Chang, *Opt. Lett.* **10**, 37 (1985).
9. H.-M. Tzeng, K. F. Wall, M. B. Long, R. K. Chang, *ibid.* **9**, 499 (1984).
10. H.-M. Tzeng, K. F. Wall, M. B. Long, R. K. Chang, *ibid.*, p. 273.
11. P. Chýlek, J. T. Kiehl, M. K. W. Ko, *Appl. Opt.* **17**, 3019 (1978).
12. A. Ashkin and J. M. Dziedzic, *Phys. Rev. Lett.* **38**, 1351 (1977).
13. H.-M. Tzeng, M. B. Long, R. K. Chang, P. W. Barber, *Opt. Lett.* **10**, 209 (1985).
14. H. Lamb, *Hydrodynamics* (Dover, New York, 1945), pp. 475 and 639.

15. Supported in part by the Air Force Office of Scientific Research (contract F49620-85-K-0002) and the Army Research Office (contract DAAG29-85-K-0063).

21 June 1985; accepted 30 September 1985

Indirect Observation by ^{13}C NMR Spectroscopy of a Novel CO_2 Fixation Pathway in Methanogens

JEREMY N. S. EVANS, CYNTHIA J. TOLMAN, MARY F. ROBERTS

High-field carbon-13 nuclear magnetic resonance (NMR) spectroscopy has been used to monitor the isotopic dilution of doubly carbon-13–labeled precursors for 2,3-cyclopyrophosphoglycerate, a novel primary metabolite that occurs in certain methanogens. A unique carbon dioxide fixation pathway that gives rise to asymmetric labeling of acetyl coenzyme A has been demonstrated in *Methanobacterium thermoautotrophicum*. The effect of selected metabolic inhibitors on the labeled species in the pathway has been examined by NMR. These techniques establish a general, sensitive method for the delineation of convergent biosynthetic pathways.

METHANOGENS ARE ARCHAEBACTERIA (*1*) that can produce methane by reduction of carbon dioxide with hydrogen. This reaction provides the cells with energy. The fixation of CO_2, which is the sole carbon source for autotrophic methanogens, into cellular material initially occurs by formation of acetyl coenzyme A (CoA) (*2–4*), and this has been shown (*4, 5*) to be derived from CO_2 via two different pathways. Neither the Calvin cycle (*6*) nor the reductive tricarboxylic acid cycle (*7*) operates in CO_2 assimilation in the methanogenic autotroph *Methanobacterium thermoautotrophicum* (*2, 8, 9*). Instead, carbon assimilation takes place by a third CO_2 fixation pathway, in which 90 percent of the total CO_2 is converted into CH_4 and the remainder is used largely for acetyl CoA synthesis (*10*). The novel metabolite 2,3-cyclopyrophosphoglycerate (CPP) is formed rapidly at high intracellular concentrations (10 m*M*)(*11*). Recent carbon-13 (^{13}C) nuclear magnetic resonance (NMR) studies have shown that CO_2, acetate, pyruvate, and phosphoenolpyruvate (PEP) serve as biosynthetic precursors for CPP and that CPP occupies a central role in carbohydrate metabolism (*12*).

Methanobacterium thermoautotrophicum cells fed with $^{13}CO_2$ exhibit intense resonances at 70.1 and 78.6 parts per million (ppm); these peaks were assigned to C-3 and C-2 of CPP (*11*). Furthermore, [1-^{13}C]acetate is incorporated specifically into C-2 of CPP, [2-^{13}C]acetate into C-3 of CPP, and [1-^{13}C]pyruvate into C-1 of CPP. Since CPP is rapidly and intensely labeled by $^{13}CO_2$, [^{13}C]acetate, and [^{13}C]pyruvate, it is a suitable probe for reactions leading up to C_3 units. In particular, with the use of doubly labeled precursors, ^{13}C NMR can be employed to detect any scrambling of C_2 or C_3 units that occurs in *Mb. thermoautotrophicum*. The spin-spin coupling ($^1J_{CC}$) of [2,3-$^{13}C_2$]CPP is thus diagnostic for the integrity of a C_2 precursor such as [1,2-$^{13}C_2$]acetate. If label scrambling were to

Department of Chemistry, Massachusetts Institute of Technology, Cambridge 02139.